Design, synthesis and structure of new potential electrochemically active boronic acid-based glucose sensors †

Jens Chr. Norrild *‡[a] and Inger Søtofte [b]

[a] *University of Copenhagen, Department of Chemistry, Laboratory for General and Organic Chemistry, Universitetsparken 5, DK-2100 Copenhagen, Denmark. E-mail: jcn@torsanadd.com*
[b] *Technical University of Denmark, Department of Chemistry, DK-2800 Kgs.Lyngby, Denmark. E-mail: is@kemi.dtu.dk; Fax: +45 45 88 31 36*

In the course of our investigations on new boronic acid based carbohydrate sensors three new boronic acids **3**, **7** and **11** containing a ferrocene moiety were synthesised. Their design includes an intramolecular B–N bonding motif in order to facilitate binding at physiological pH. We report the synthesis of the compounds and our investigations on glucose complexation as studied by ^{13}C NMR spectroscopy. The crystal structure of 2,4,6-tris[2-(*N*-ferrocenylmethyl-*N*-methylaminomethyl)phenyl]boroxin (**13**) (boroxin of boronic acid **3**) (boroxin = cyclotriboroxane) was obtained and compared with structures obtained of 2,4,6-tris[2-(*N,N*-dimethylaminomethyl)phenyl]boroxin (**14**) and 2,2-dimethyl-1,3-diyl[2-(*N,N*-dimethylaminomethyl)phenyl]boronate (**15**). The structure of **13** shows the existence of intramolecular B–N bonds in the solid phase.

Introduction

Lately there has been considerable interest in boronic acid based carbohydrate sensors as potential substitutes for commercial enzyme based sensors. Several boronic acid based sensor molecules have been published for which the sensory principle covers a broad range of techniques such as fluorescence,[1,2] UV-Vis absorption,[3,4] circular dichroism[5,6] and electrochemistry. The latter technique combined with boronic acids, however, has not been as extensively investigated and one finds only a few publications on the subject.[7,8] One of these, from Shinkai's group, reported on the properties of the chiral ferroceneboronic acid **17**, Fig. 1.
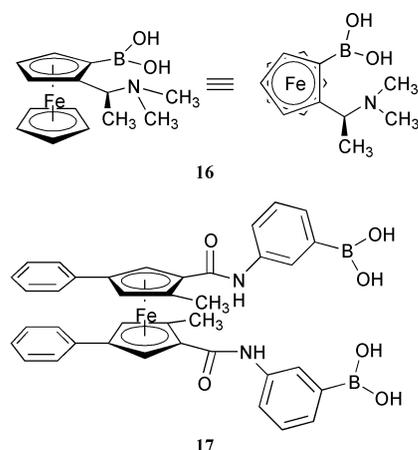

Fig. 1 Previously published ferrocene containing boronic acids.

This compound and its mirror image were shown to give a strong response to D-sorbitol but gave none or very week responses to D-glucose at neutral pH. Recently we published our further investigations of **16**[9,10] which showed that the earlier anticipated intramolecular B–N bond in this molecule does not exist. If, however, intramolecular B–N bonds can be formed between a boronic acid moiety and a neighbouring amino group, this may strongly enhance binding of carbohydrates at neutral pH. This is due to formation of species like II (Scheme 1) which exists in a pH-range from approximately
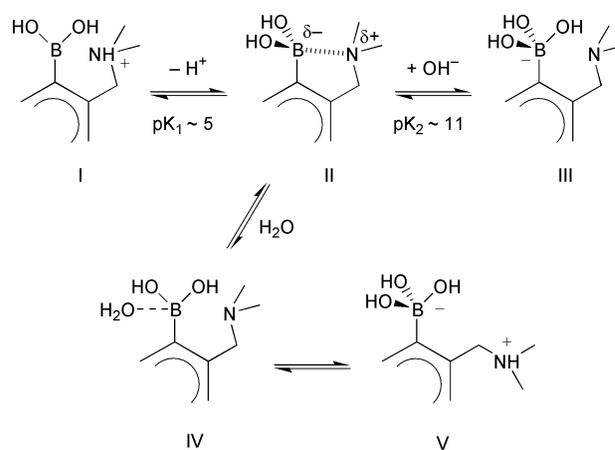
Scheme 1

5 to 11 and which holds partial tetrahedral boron atoms. These are known to bind diols more strongly than their "acidic" trigonal planar counterparts. In the absence of the B–N interaction strong binding normally requires pH-values above 9.

The reversible B–N bond formation, which fails for ferroceneboronic acid **16**, is well documented both in solution[11–13] and in the solid phase[14,15] when the structural motif as in II (Scheme 1) is attached to a 6-membered benzene system. This motif, originally developed by Wulff for other purposes,[16] has successfully been used by Shinkai's group in the design of a glucose selective fluorescent sensor molecule.[17,18]

Scheme 2

Shinkai's and our own studies have shown that two boronic acids placed in an optimised geometry are needed in order to strongly bind to glucose. We have in several studies consistently shown glucose in aqueous solution to be bound as a 1,2-3,5,6-α-D-glucofuranose bisboronate, where the second binding site may vary between (3,5), (5,6) and (3,5,6) depending on the geometry of the sensor molecules.[1,19,20] From this knowledge we designed and synthesised the new ferrocene bisboronic acids **7** and **11** as well as the monoboronic acid analogue **3** (Scheme 2), which all utilize ferrocene both as structural element and as functional group.[21] Here we report the synthesis of these new molecules as well as our preliminary results from binding studies and electrochemical measurements.

Results and discussion

Synthesis

The syntheses of the new boronic acids **3**, **7**, and **11** were performed as shown in Scheme 2. The key intermediates are the (methylaminomethyl)ferrocenes **2**, **6**, and **10** which were easily obtained in good yields by reductive aminations of their aldehyde precursors. The monoamine **2** was previously described but of the bis-amines **6** and **10**, only the latter is mentioned in a patent.[22] Alkylation of the amines with protected *o*-bromomethylphenylboronic acid **12** proceeded fast but in some cases minor amounts of over-alkylated product were observed. Therefore we added **12** slowly at 0 °C, and base was only added after final addition of the boronic acid. Deprotection went smoothly under slightly alkaline conditions by stirring at room temperature in a water–EtOAc mixture. The free boronic acids **3**, **7**, and **11** were easily purified and obtained in good yields. Analyses showed in all cases the compounds to be isolated as partial anhydrides. In the case of monoboronic acid **3**, this compound could be recrystallized from EtOAc–hexane to give orange needles. An X-ray investigation revealed the structure to be a cyclic

anhydride (a boroxin) as shown in Scheme 3 and Fig. 4. The crystal structure reveals three B–N bonds of approximately 1.8 Å to exist in the solid phase (see Scheme 3), thus indicating

Scheme 3

a similar structural motif to exist in solution. The crystal structure of **13** together with two comparable structures are treated in a later section.

Glucose complexes

Complexes between α-D-glucose and the new ferroceneboronic acids were investigated by NMR and mass spectrometry. ^{1}H NMR gave only limited information due to overlap of the carbohydrate signals and absorptions in the ferroceneboronic acids. On the other hand ^{13}C NMR on samples with ferroceneboronic acid and uniformly ^{13}C labelled glucose gave the spectra as depicted in Fig. 2 only showing signals from the
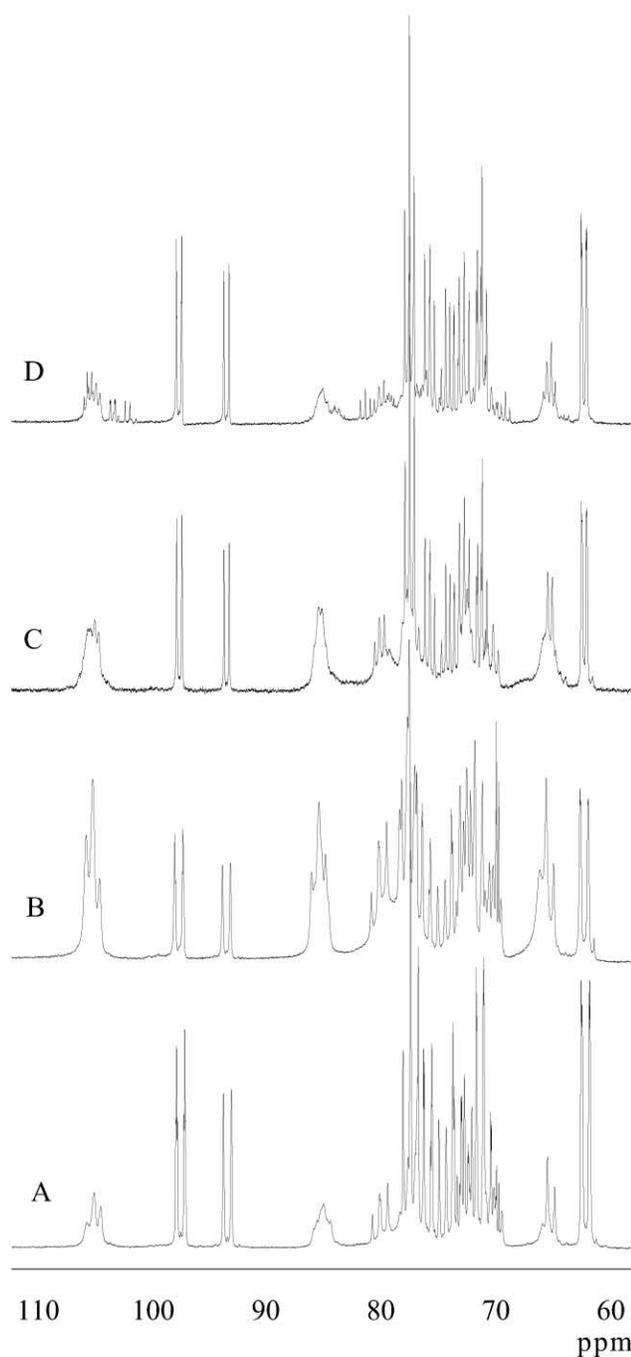
sugar part.[23] As can be seen from the spectra, all three boronic acids give rise to glucose complexes in a mixture with the free glucopyranoses, the absorptions from the complexes being considerably broadened. All complexes showed absorptions from C-1 around 105 ppm. Together with the absorptions at ~85 ppm this strongly suggests prevalent complexation of the furanose form of glucose in agreement with our previous

investigations.[1,19,20,24] As glucose has two binding sites for boronic acids, the monoboronic acid **3** should be expected to give a 1 : 2 complex (glucose to boronic acid) whereas the bisboronic acids may give either 1 : 1 or polymeric complexes. From a spectrum of bisboronic acid **11** and glucose our first conclusion was that the broad signals observed were due to polymeric species, but as the spectra of monoboronic acid **3** and glucose gave similar broad lines we concluded that the carbon atoms within the complexes obviously had very short T_2 relaxation times compared to those of the free carbohydrate. In an attempt to "filter out" any polymer present in the 1 : 1 mixture of **11** and glucose, we performed a standard Carr–Purcell–Meiboom–Gill (CPMG) T_2 experiment without phase cycling and with varying relaxation times. This preliminary experiment showed that there seems to be some polymeric species present but surely also a mixture of smaller complexes as the C-1 signal at ~105 ppm appears as a broad triplet and not as a doublet as should be expected. In the spectrum shown in Fig. 2, entry C, the C-6 signal at 65 ppm appears as a doublet of 40 Hz with an underlying broad signal. This coupling constant may indicate that OH-6 does not take part in the binding,[19] thus implying a (3,5) secondary binding site in the major complex. Possible structures of the 1 : 1 complexes between **11** and glucose are shown in Fig. 3 but we
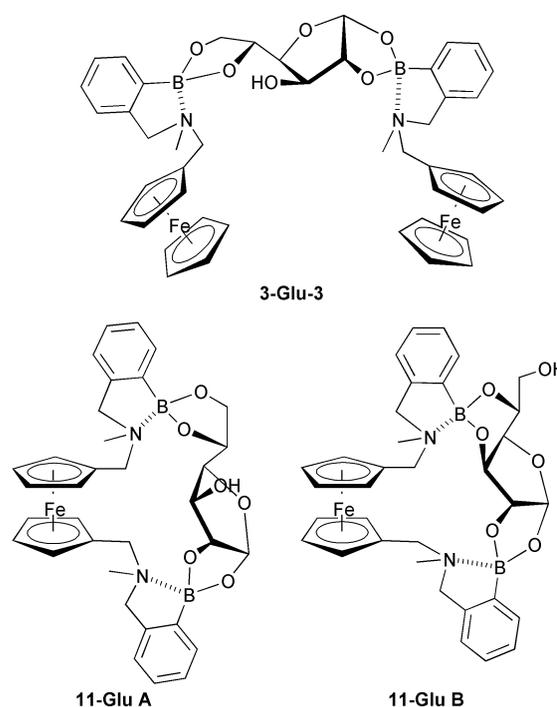

3-Glu-3

11-Glu A   **11-Glu B**

Fig. 3 Selected feasible structures of 1 : 1 and 2 : 1 complexes. Stereocenters at boron and nitrogen atoms make several isomeric structures feasible.

cannot, at this stage, draw any final conclusions concerning the structures.

For the 1 : 2 complex between glucose and **3**, a spectrum obtained at 1 °C revealed a splitting of the broad "triplet" C-1 signal at 25 °C (Fig. 2, entry B) into multiple doublets with two major signals having $^1J_{C1-C2}$ coupling constants of approximately 34 and 35 Hz in agreement with 1,2-bound boronates.[19] Furthermore the observed C-6 doublet at ~65 ppm ($^1J_{CC}$ ~ 41 Hz) with an underlying broad signal sharpened into a distorted triplet with apparent $^1J_{C-C}$ coupling constants of 40 and 34 Hz. From this, until now, limited information we cannot safely assign the major secondary binding site for these complexes.

The appearance of multiple peaks from the **3**–glu–**3** complex may be ascribed to the fact that mixtures of several diastereomeric complexes are to be expected due to the variable stereo-

chemistry around the tetrahedral boron and nitrogen atoms (compare Fig. 3). This is of course also the case for glucose complexes of **7** and **11**, whether polymeric or not, and especially from the spectrum of a 1 : 1 mixture of **7** and glucose, the presence of several complexes is evident (see Fig. 2 entry D). The presence of polymer complexes for the latter compounds was furthermore envisioned by slow evaporation of the solvent giving rise to gel formation.

To unambiguously prove the presence of 1 : 1 complexes for bisboronic acids **7** and **11** and 1 : 2 complexes for monoboronic acid **3** we performed a FAB mass spectrometric analysis (see Experimental). In 1 : 1 mixtures of glucose and **7** and **11** respectively, we were able to prove the presence of $m/z = 649$. This mass corresponds to $MH^+ = [C_{34}H_{39}B_2FeN_2O_6]^+$ expected for the two isomeric 1 : 1 complexes. Isotope patterns were in agreement with the calculated one. For the 1 : 2 mixture of glucose and **3** a peak at $m/z = 835$ appeared ($MH^+ = [C_{44}H_{49}Fe_2N_2B_2O_6]^+$) with a somewhat distorted isotope pattern which was ascribed to overlap from the oxidised compound with $m/z = 834$. FAB(−) gave only $[M−H]^-$ ($m/z = 833$) as expected with the right isotope pattern.

Preliminary electrochemical measurements have shown the reversible oxidation–reduction of **3**, **7**, and **11** with $E^{o\prime}$ values of 0.59, 0.68 and 0.69 V respectively (ref. ferrocene/aceto-nitrile = 0.63 V). Currently, investigations are in progress of the electrochemical response of the sensor molecules in solution to glucose and other carbohydrates.

X-Ray crystallography

The crystal structure of 2,4,6-tris[2-(*N*-ferrocenylmethyl-*N*-methylaminomethyl)phenyl]boroxin (**13**) (See Scheme 3 and Fig. 4) was obtained and compared with structures obtained
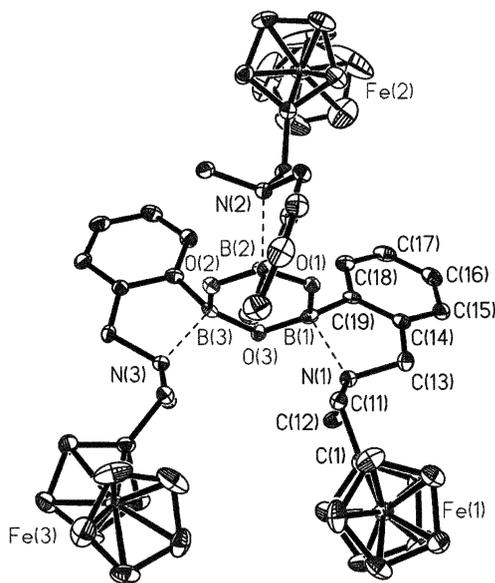
Fig. 4 View of 2,4,6-tris[2-(*N*-ferrocenylmethyl-*N*-methylamino-methyl)phenyl]boroxin (**13**). Elipsoids are drawn at a 50% probability level. The numbering of the atoms of the cyclopentadienyl ring (C(2)–C(10)) is omitted for clarity. Also, the hydrogen atoms have been omitted for clarity.

of 2,4,6-tris[2-(*N*,*N*-dimethylaminomethyl)phenyl]boroxin (**14**) and 2,2-dimethyl-1,3-diyl[2-(*N*,*N*-dimethylaminomethyl)phen-yl]boronate (**15**) (See Scheme 3 and Fig. 5 and 6). Crystal data for the three compounds are listed in Table 1 and selected bond lengths, angles and torsion angles are listed in Tables 2–4. The labelling of the atoms in the molecules is shown in Fig. 4–6. Bond lengths and angles of the structures are in the expected ranges.

In all three structures there are intramolecular B–N bonds. In boroxin **13** the three B–N bonds are 1.829(4), 1.842(3) and
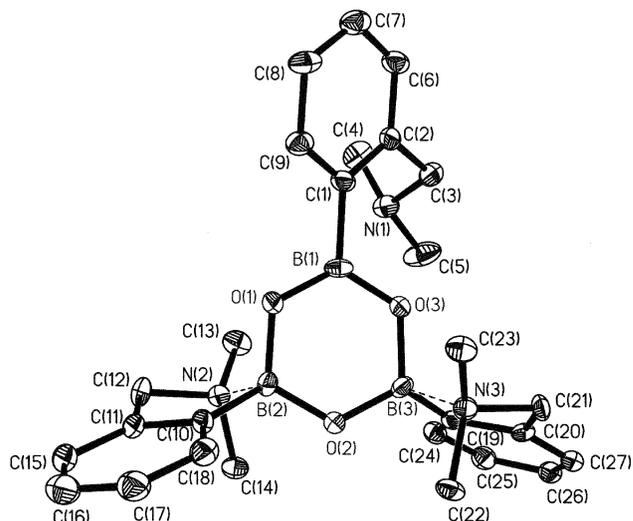
Fig. 5 View of 2,4,6-tris[2-(*N*,*N*-dimethylaminomethyl)phenyl]-boroxin (**14**). Elipsoids are drawn at a 50% probability level. The hydrogen atoms have been omitted for clarity.

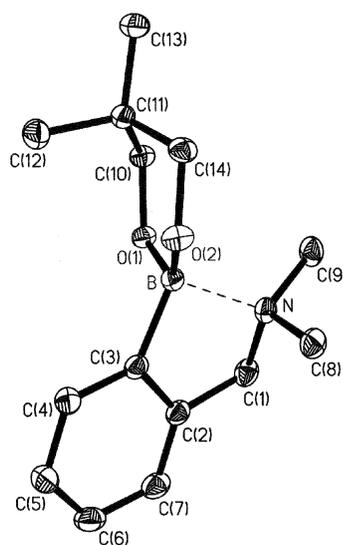**Fig. 6** View of 2,2-dimethyl-1,3-diy1[2-(*N*,*N*-dimethylaminomethyl)-pheny1]boronate (**15**). Elipsoids are drawn at a 50% probability level. The hydrogen atoms have been omitted for clarity.

1.775(3) Å, respectively. In **14** only two B–N bonds [B(2)–N(2) of 1.765(4) and B(3)–N(3) of 1.756(4) Å] are found. There is no B–N bond between B(1) and N(1), the B · · · N distance being 3.171(4) Å. In boronate **15** the B–N bond is 1.765(2) Å. The B–N bonds in the present structures are in agreement with those found in 9-[2-(dimethylaminomethyl)phenyl]-9-borabicyclo[3.3.1]nonane, 9-[2-(diethylaminomethyl)phenyl]-9-borabicyclo[3.3.1]nonane and 2-[2-(dimethylaminomethyl)-phenyl]-4,4-diphenyl-1,3,2-dioxaborolane,[14] 2,6-bis(*N*,*N*-di-methylaminomethyl)phenylboronate[25] and 2-{2-[1-(dimethyl-amino)-1-methylethyl]phenyl}-4,4-diphenyl-1,3,2-dioxaboro-lane[13] except for the two of 1.829(4) and 1.842(3) Å, which are somewhat longer.

The tetrahedral character ($THC_{DA}[\%]$) of the boron atoms in the structures has been calculated from a formula introduced by Höpfl, that includes all six bond angles at the boron atom.[26] The N–B bond length (Å) and the calculated tetrahedral character of the various boron groups are summarised in Table 5. The values found in the present structures are in agreement with those listed by Höpfl for related compounds.[26]

The torsion angles C–C–N–B about the C–N bonds are simi-lar in the three structures and in the range 31.0(3)–35.8(2)°, whereas for the torsion angles C–C–B–N about the C–B bonds

Table 1 Crystallographic data for compounds **13**, **14** and **15**

	13	**14**	**15**
Formula	$C_{57}H_{60}B_3Fe_3N_3O_3$	$C_{27}H_{36}B_3O_3$	$C_{14}H_{22}BNO_2$
Fw	1035.06	483.02	247.14
Temp. T/K	120(2)	120(2)	120(2)
Cryst. system	Triclinic	Orthorhombic	Monoclinic
Space group	$P\bar{1}$	$P2_12_12_1$	$P2_1/c$
a/Å	10.6303(11)	8.9765(3)	9.0771(1)
b/Å	15.1238(15)	14.6975(4)	12.1030(2)
c/Å	15.700(2)	19.6627(6)	12.8969(1)
α/°	81.784(2)	—	—
β/°	72.121(2)	—	103.667(1)
γ/°	81.651(2)	—	—
V/Å³	2363.7(4)	2594.1(1)	1376.74(3)
Z	2	4	4
$\mu_{(MoK\alpha)}$/mm^{-1}	0.959	0.078	0.077
Cryst. colour	Yellow–brown	Colourless	Colourless
Cryst. size/mm	$0.33 \times 0.23 \times 0.09$	$0.34 \times 0.10 \times 0.08$	$0.35 \times 0.13 \times 0.10$
Meas. reflns	16807	17671	9135
Unique reflns	11761	3843	3510
Reflns with $[I > 2\sigma(I)]$	7920	2908	2729
R(int)	0.0294	0.0827	0.0506
Refined param.	622	325	343
$R1^a$ (obs. data)	0.0479	0.0592	0.0528
$wR2^b$ (all data)	0.1116	0.1260	0.1246

^{a} $R1 = \Sigma ||F_o| - |F_c||/\Sigma|F_o|$. ^{b} $wR2 = [\Sigma w|F^2_o - F^2_c|^2/\Sigma wF_o^4]^{1/2}$

Table 2 Selected bond lengths (in Å), bond angles (in °) and torsion angles (°) for **13**

	Fe(1)	Fe(2)	Fe(3)
C(1/A/B)–C(11/A/B)	1.507(4)	1.502(3)	1.500(3)
C(11/A/B)–N(1/2/3)	1.483(3)	1.484(3)	1.486(3)
N(1/2/3)–B(1/2/3)	1.829(4)	1.842(3)	1.775(3)
C(13/A/B)–C(14/A/B)	1.507(3)	1.506(3)	1.509(3)
C(19/A/B)–B(1/2/3)	1.614(4)	1.610(4)	1.629(4)
B(1/2/3)–O(1/1/2)	1.421(3)	1.417(3)	1.423(3)
B(1/2/3)–O(3/2/3)	1.413(3)	1.406(3)	1.415(3)
C(2/A/B)–C(1/A/B)–C(11/A/B)	127.6(2)	126.1(2)	126.2(2)
C(5/A/B)–C(1/A/B)–C(11/A/B)	124.8(2)	126.5(2)	126.5(2)
N(1/2/3)–C(11/A/B)–C(1/A/B	113.2(2)	114.0(2)	114.3(2)
C(12/A/B)–N(1/2/3)–B(1/2/3)	108.2(2)	107.4(2)	109.5(2)
C(11/A/B)–N(1/2/3)–B(1/2/3)	112.1(2)	112.4(2)	111.2(2)
C(13/A/B)–N(1/2/3)–B(1/2/3)	103.0(2)	102.8(2)	103.4(2)
N(1/2/3)–C(13/A/B)–C(14/A/B)	105.1(2)	105.2(2)	105.6(2)
C(14/A/B)–C(19/A/B)–B(1/2/3)	113.1(2)	113.4(2)	111.4(2)
C(18/A/B)–C(19/A/B)–B(1/2/3)	130.1(2)	129.0(2)	131.5(2)
O(3/2/3)–B(1/2/3)–O(1/1/2)	117.5(2)	117.6(2)	116.2(2)
O(3/2/3)–B(1/2/3)–C(19/A/B)	117.3(2)	117.1(2)	118.0(2)
O(1/1/2)–B(1/2/3)–C(19/A/B)	113.9(2)	114.7(2)	112.6(2)
O(3/2/3)–B(1/2/3)–N(1/2/3)	107.0(2)	106.6(2)	108.8(2)
O(1/1/2)–B(1/2/3)–N(1/2/3)	103.4(2)	103.5(2)	103.9(2)
C(19A/B)–B(1/2/3)–N(1/2/3)	93.0(2)	92.3(2)	93.7(2)
B(2/2/1)–O(1/2/3)–B(1/2/3)	121.9(2)	121.9(2)	121.3(2)
B(1/2/3)–N(1/2/3)–C(13/A/B)–C(14/A/B)	−34.9(2)	−35.8(2)	34.3(2)
C(14/A/B)–C(19/A/B)–B(1/2/3)–N(1/2/3)	−19.9(2)	−20.7(3)	24.3(2)
N(1/2/3)–C(13/A/B)–C(14/A/B)–C(19/A/B)	24.2(3)	24.7(3)	−19.9(3)
C(14/A/B)–C(19/A/B)–B(1/2/3)–O(3/2/3)	−130.8(2)	−130.7(2)	137.9(2)
C(14/A/B)–C(19/A/B)–B(1/2/3)–O(1/1/2)	86.2(3)	85.4(3)	−82.4(3)
C(2/A7B)–C(1/A/B)–C(11/A/B)–N(1/2/3)	64.5(3)	−79.8(3)	92.9(3)
C(5/A/B)–C(1/A/B)–C(11/A/B)–N(1/2/3)	−108.2(3)	99.2(3)	−87.4(3)
C(1/2/3)–C(11/A/B)–N(1/2/3)–C(12/A/B)	46.0(3)	62.3(3)	−54.6(3)
C(1/1/3)–C(11/A/B)–N(1/2/3)–C(13/A/B)	−76.9(3)	−61.7(3)	68.3(3)
C(13/A/B)–N(1/2/3)–B(1/2/3)–C(19/A/B)	32.7(2)	33.7(2)	−34.7(2)

$$\text{THC}_{\text{Donor-accept}}[\%] = \text{THC}_{\text{DA}}[\%] = \left[1 - \frac{\sum\limits_{n=1-6} |109.5 - \theta_n|°}{90°} \right] \times 100 \quad (1)$$

the torsion angle of 25.7(2)° in **15** is slightly larger and the torsion angles of 14.6(3) and 16.2(3)° in **14** are smaller than those found in **13** [19.9(2)–24.3(2)°]. The distances between the nitrogen atoms and the least-squares plane through the other four atoms in the N–C–C–C–B rings are 0.605(4), 0.621(4) and 0.606(4) Å, respectively, for the three moieties

Table 3 Selected bond lengths (in Å), bond angles (in °) and torsion angles (°) for **14**

B(1/2/3)–O(1/2/2)	1.363(4)	1.413(4)	1.413(4)
B(1/2/3)–O(3/1/3)	1.360(4)	1.454(4)	1.455(4)
B(1/2/3)–C(1/10/19)	1.577(5)	1.615(5)	1.609(5)
B(2/3)–N(2/3)		1.765(4)	1.756(4)
O(3/2/2)–B(1/2/3)–O(1/1/3)	122.0(3)	115.8(3)	115.5(3)
O(1/2/2)–B(1/2/3)–C(1/10/19)	118.4(3)	117.1(3)	118.3(3)
O(3/1/3)–B(1/2/3)–C(1/10/19)	119.3(3)	113.1(3)	112.4(3)
B(1/3/1)–O(1/2/3)–B(2/2/3)	120.7(3)	123.7(3)	121.2(3)
O(1/3)–B(2/3)–N(2/3)		104.1(2)	103.5(2)
O(2/2)–B(2/3)–N(2/3)		107.8(3)	107.7(2)
C(10/19)–B(2/3)–N(2/3)		95.7(2)	96.2(2)
C(2/11/20)–C(1/10/19)–B(1/2/3)	124.0(3)	111.8(3)	112.0(3)
C(9/18/24)–C(1/10/19)–B(1/2/3)	118.2(3)	131.0(3)	130.6(3)
N(1/2/3)–C(3/12/21)–C(2/11/20)	111.8(3)	105.3(3)	105.3(3)
C(12/21)–N(2/3)–B(2/3)		104.0(2)	104.3(2)
C(13/23)–N(2/3)–B(2/3)		113.6(2)	112.8(2)
C(14/22)–N(2/3)–B(2/3)		109.2(2)	110.4(2)
C(11/20)–C(12/21)–N(2/3)–B(2/3)		−32.5(3)	−31.0(3)
N(2/3)–B(2/3)–C(10/19)–C(11/20)		−16.2(3)	−14.6(3)
C(1/10/19)–C(2/11/20)–C(3/12/21)–N(1/2/3)	61.6(4)	23.9(4)	23.5(3)
O(1/2/2)–B(1/2/3)–C(2/10/19)–C(3/11/20)	−151.3(3)	−129.6(3)	−128.5(3)
O(3/1/3)–B(1/2/3)–C(2/10/19)–C(3/11/20)	34.5(5)	91.8(3)	92.8(3)

Table 4 Selected bond lengths (in Å), bond angles (in °) and torsion angles (°) for **15**

O(1)–C(10)	1.422(2)
O(1)–B	1.438(2)
O(2)–C(14)	1.417(2)
O(2)–B	1.425(2)
N–B	1.765(2)
C(3)–B	1.610(2)
C(10)–O(1)–B	120.20(12)
C(14)–O(2)–B	118.49(12)
C(9)–N–B	115.44(12)
C(8)–N–B	109.54(12)
C(1)–N–B	102.44(11)
N–C(1)–C(2)	105.00(13)
C(4)–C(3)–B	131.04(15)
C(2)–C(3)–B	110.96(14)
O(2)–B–O(1)	117.66(14)
O(2)–B–C(3)	116.56(13)
O(1)–B–C(3)	110.03(13)
O(2)–B–N	108.60(12)
O(1)–B–N	106.59(12)
C(3)–B–N	94.36(11)
B–N–C(1)–C(2)	−35.6(2)
C(2)–C(3)–B–N	−25.69(15)
N–C(1)–C(2)–C(3)	20.8(2)
C(2)–C(3)–B–O(2)	−139.0(2)
C(2)–C(3)–B–O(1)	83.7(2)

Table 5 The N–B length (Å) and the tetrahedral character, THC_DA(%) of the various boron groups

Structure		d(B–N)	THC$_{DA}$
13			
Around	B(1)	1.829(4)	49.7
	B(2)	1.842(3)	47.8
	B(3)	1.775(3)	55.1
14			
Around	B(1)	3.171(4)	–
	B(2)	1.765(4)	57.3
	B(3)	1.756(4)	56.9
15		1.765(2)	61.4

13 they are in the range 19.9(3)–24.7(3)° and in **15** the torsion angle is 20.8(2). Except for the torsion angle of 61.6(4)° and the displacement of N(1) of 1.255(5) Å in **14**, the values are in agreement with those found in 9-[2-(dimethylaminomethyl)-phenyl]-9-borabicyclo[3.3.1]nonane, 9-[2-(diethylamino-methyl)phenyl]-9-borabicyclo[3.3.1]nonane and 2-[2-(dimethyl-aminomethyl)phenyl]-4,4-diphenyl-1,3,2-dioxaborolane.[14] In the structure we find no intermolecular interactions which can explain the different conformation of one of the dimethyl-aminomethyl groups.

In the boroxin ring of **13** the B–O bonds are in the range 1.406(3)–1.423(3) Å which is in agreement with the B–O bonds found around B(2) and B(3) in **14** (1.413(4) to 1.455(4) Å) and in the boronate ring of **15** (1.425(2) and 1.438(2) Å). As could be expected, the B(1)–O bonds in **14** of 1.363(4) and 1.360(4) Å are shorter than those around boron atoms with more sp^3-character and consequently partial negative charge. In **14** the O–B(1)–O angle is 122.0(3)° compared to values of 115.5(3) to 117.7(1)° around the other boron atoms in **13**, **14** and **15**.

In boroxin **13** the B–C(phenyl) bonds of 1.610(4)–1.629(4) Å and the angles between the least-squares plane of the boroxin ring and the phenyl rings attached at B(1), B(2) and B(3) of 70.28(9), 73.81(9) and 77.78(8)°, respectively are similar to those found for B(2) and B(3) [75.02(9) and 77.06(8)°] in **14**. Around the B(1) atom in **14** the B–C(phenyl) bond is 1.577(5) Å and the angle between the boroxin and the B1-phenyl is 38.86(12)°.

The B–O bond lengths and the B–C(phenyl) bonds in **13** and **14** are all, except for B(1)–O bonds in **14**, longer than the values found in (4-MeC$_6$H$_4$)$_3$B$_3$O$_3$,[27] where the B–O bonds are 1.383(4) and 1.383(4) Å, the O–B–O angles are in the range 117.9(4)–119.4(3)° and the B–C(phenyl) bonds 1.521(6)–1.543(4) Å. In the latter structure the plane of the boroxin ring and the phenyl rings are essentially co-planar.

In the boronate ring of **15** the B–O bonds are slightly longer (1.425(2) and 1.438(2) Å) and the B–C bond of 1.610(2) Å is longer than those found in N-(4-nitrophenylmethylidene)-5-methyl-2-phenyl-1,3-dioxa-2-boracyclohexan-5-amine N-oxide[28] and 5-methyl-5-nitro-2-phenyl-1,3-dioxa-2-boracyclo-hexane[29] [B–O: 1.367(3), 1.358(3) and B–C: 1.559(4) Å]. The bond angle O–B–O of 117.7(1)° is smaller than those of 122.8(2) and 122.4(3)° found in the latter compounds.[28,29]

The six-membered ring in the present structure has a chair conformation, whereas in N-(4-nitrophenylmethylidene)-5-methyl-2-phenyl-1,3-dioxa-2-boracyclohexan-5-amine N-oxide[28] and 5-methyl-5-nitro-2-phenyl-1,3-dioxa-2-boracyclo-

in **13**, 1.255(5), 0.540(5) and 0.511(5) Å, respectively, in **14** and 0.636(2) Å in **15**.

As mentioned above, the N(1)Me$_2$ group in boroxin **14** is in a different conformation compared to the other two NMe$_2$ groups. The torsion angles N–C–C–C(attached to B) for N(1), N(2) and N(3) are 61.6(4), 23.9(4) and 23.5(3)°, respectively. In

hexane[29] the rings have a "semi-planar" (envelope) conformation.

In **13** the Fe–C bond lengths are in the range 2.004–2.047 Å and the coordination around the Fe(II)-ions is in agreement with the results found in similar compounds, *e.g.* in 2-(*N,N*-dimethylaminoalkyl)ferroceneboronic acids and their diol derivatives.[9] The cyclopentadienyl rings of the ferrocene [Fe(1) and Fe(3)] moieties are almost eclipsed, whereas in the Fe(2) part they are almost staggered. The rings are planar and the angles between them are 1.8(2)° in the Fe(1) and the Fe(3) moieties and 0.9(2)° in the Fe(2) group. The distances from the planes of the cyclopentadienyl rings to Fe(II)-ions are in the range 1.637–1.649 Å. The bond lengths, angles and torsion angles of the three moieties are quite similar. In the Fe(2) and Fe(3) groups the ethyl carbon atoms C(11A) and C(11B) are located in the plane of the substituted cyclopentadienyl rings, whereas in the Fe(1) moiety the carbon atom C(11) is 0.131(4) Å above the plane. This is in agreement with what was found in 2-(*N,N*-dimethylaminoalkyl)ferroceneboronic acids and their diol derivatives.[9] For all three structures presented here, as expected, there are no classic hydrogen bonds in the structures and the C–H $\cdots$ A bonds are all weak.

Conclusion

In conclusion, we have deduced a straightforward synthesis of three new promising glucose sensors based on boronic acid-appended ferrocenes[21] and evaluated their glucose binding abilities. For the three sensor molecules the formation of mixtures of glucofuranose complexes has been concluded, however determination of detailed structures of the complexes and their stability constants was precluded by the very broad lines observed, even when cooling to ~0 °C. We ascribe the line broadening phenomenon to internal equilibria (*via* B–N bond breaking/formation) between various complexes as *e.g.* 11-Glu A and B (Fig. 3) or between similar structures with inverted nitrogen atoms.

In contrast to the published boronic acids **16** and **17** (Fig. 1), the crystal structure of **13** (the boroxin of **3**) proves that our new sensor design favours B–N interactions which allow strong sugar binding at physiological pH.

In our laboratory, we have initiated a study of the electrochemical behaviour of the new sensor molecules on which we will report in due course. For future development of the boronic acid-appended ferrocenes presented here, we envision these molecules to be easily converted to *e.g.* *N*-alkyl analogues incorporating functional groups for solid phase immobilisation *e.g.* onto an electrode.

Experimental

^{1}H and ^{13}C NMR spectra were recorded at 25 °C at 400 MHz and 100 MHz respectively. Chemical shifts are reported in ppm. The spectra are referenced as follows: CD_3OD, ^{13}C referenced internally to CD_3OD = 49.0 ppm and ^{1}H to CHD_2OD = 3.30 ppm. Evaporations were performed *in vacuo* on a rotary evaporator at 40–50 °C. Melting points are uncorrected. Microanalyses were performed by Microanalytical Laboratory, University of Copenhagen.

Mass spectra were obtained on a Jeol JMS-HX/HX110A tandem mass spectrometer. Analyses for FAB investigations were prepared by dissolving the boronic acid (7.5 mg (14 μmol) for **7** and **11** and 9.8 mg (27 μmol) for **3**) + glucose (non-labeled 2.5 mg, 14 μmol) in CH_3OH (0.2 g) + two drops of water. HRMS analyses of **3**, **7** and **11** were made after treatment of a few milligrams of each product with 2,2-dimethylpropane-1,3-diol in toluene (1 mL). The toluene was heated to 80 °C and concentrated to 1/10 of the volume in a stream of nitrogen.

Samples for NMR were made as follows. Sensor molecules **3**, **7**, or **11** (0.028 mmol) and UL-[13]C_6 α-D-glucose (0.028 mmol)

were dissolved in CD_3OD (0.5 g), D_2O (0.2 g), DMSO (0.1 g). (DMSO was added only to speed up dissolution of the sensor molecules). For the 1 : 2 mixture of glucose and **3** 0.056 mmol of **3** was used. Long time stability of the samples at RT was observed.

Materials

All chemicals used were of reagent grade and all solvents were of HPLC grade. THF was distilled from Na–benzophenone. Compound **12** was prepared analogously to Shinkai *et al.*[17] but was distilled in vacuum before use. UL [13]C_6 labelled α-D-glucose was obtained from Cambridge Isotope Laboratories.

X-Ray crystallography

The crystals of the compounds were cooled to 120 K using a Cryostream nitrogen gas cooler system. The data were collected on a Siemens SMART platform diffractometer with a CCD area sensitive detector. The structures were solved by direct methods and refined by full-matrix least-squares against F^2 of all data. In all the structures the non-hydrogen atoms were refined anisotropically. The hydrogen atoms could in all structures be located from electron-density difference maps but were at calculated positions using a riding model with C–H = 0.95–0.99 Å and fixed thermal parameters [$U(H) = 1.2 \times U$ for attached atom]. The absolute configuration of **3** could not be determined due to the lack of heavy atoms. Therefore, the Friedel pairs were merged. In **13** the temperature displacement parameters of C(9A) are rather high, but the position of the atom is not split up into two positions. CCDC reference numbers 169152–169154. See http://www.rsc.org/suppdata/p2/b1/b107457a/ for crystallographic files in .cif or other electronic format. Programs used for data collection, data reduction and absorption were SMART, SAINT and SADABS.[30,31] The program SHELXTL ver. 5.03[32] was used to solve the structures and for molecular graphics. PLATON[33] was used for molecular geometry calculations.

Synthesis

***N*-Methylaminomethylferrocene (2).**[34] Ferrocenecarbaldehyde (2.00 g, 9.34 mmol) was dissolved in 4.5 M MeNH$_2$ in EtOH (50 mL) in a nitrogen atmosphere. The red solution was refluxed for 1 h. After cooling to 0 °C NaBH$_4$ (0.40 g, 10.6 mmol) was added in one portion. The mixture was stirred at 0 °C for 30 min and heated to RT for 1 h. The EtOH was evaporated and the residue partitioned between water (50 mL) and ether (50 mL). The aqueous phase was extracted three times with ether (20 mL portions) and the combined ether phase was washed once with brine and dried over Na$_2$SO$_4$. Evaporation yielded 1.96 g of crude red oil. The oil was purified on an Al$_2$O$_3$ column (Act. II, 2 × 20 cm), eluent ether–ether/MeOH (5%). A minor first fraction of the yellow band was discarded and evaporation of the main fraction yielded **1** as an analytically pure red oil (1.63 g, 76%). ^{1}H NMR (CD$_3$OD) δ 4.20 (2H, t, 1.7 Hz), 4.12 (5H, s), 4.11 (2H, t, 1.7 Hz), 3.46 (2H, s), 2.32 (3H, s). ^{13}C NMR (CD$_3$OD) δ 86.3, 69.9, 69.4 (Fc$_{unsub}$), 68.9, 51.6, 35.6. Anal. Calcd. for C$_{12}$H$_{15}$FeN: C, 62.91; H, 6.60; N, 6.11. Found: C, 62.19; H, 7.78; N, 6.30%.

***N*-Methyl-*N*-[*o*-(dihydroxyboryl)benzyl]aminomethylferrocene (3).** *N*-Methylaminomethylferrocene (**2**, 200 mg, 0.87 mmol) was dissolved in dry THF (10 mL) in a N$_2$ atmosphere and cooled to 0 °C. 2,2-Dimethylpropane-1,3-diyl[(*o*-bromomethyl)phenyl]boronate (**12**, 247 mg, 0.87 mmol) was dissolved in dry THF (10 mL) and added drop by drop over 30 min to the above solution by which a precipitate forms. The mixture was stirred for a further 30 min at 0 °C and K$_2$CO$_3$ (dry, powdered) (133 mg, 1.1 equiv) was added and the mixture allowed to stir overnight at RT. The THF evaporated and the residue

partitioned between water (15 mL) and EtOAc (15 mL). The two-phase system was stirred vigorously for 4 h at RT to deprotect the boronic acid. The two phases were separated and the orange EtOAc phase was washed once with water and repeatedly stirred with water (15 mL) for 2 h. (If the last water treatment is omitted, there may be a little residual diol-protected compound left after workup). The EtOAc phase was separated, washed twice with water, with brine and finally dried over Na_2SO_4. After evaporation the resulting orange oil (311 mg) was triturated with pentane until solid formed. Filtration and washing with pentane gave after drying **3** as an orange powder 204 mg (64%). Mp. 168–173 °C. ^{1}H NMR (CD$_3$OD) δ 7.54 (1H, d, ArH), 7.22 (1H, dt, ArH), 7.17 (1H, dt, ArH), 7.07 (1H, d, ArH), 4.37 (2H, t, FcH), 4.30 (2H, t, FcH), 4.18 (5H, s, Fc$_{unsubH}$), 3.92 (2H, s, N–CH$_2$), 3.87 (2H, br s, N–CH$_2$), 2.32 (3H, s, N–CH$_3$). ^{13}C NMR (CD$_3$OD) (C–B not observed due to quadrupolar relaxation) δ 133.7, 133.6, 128.2, 128.0, 72.5, 72.5, 70.5, 70.0 (Fc$_{unsub}$), 62.5 (CH$_2$) 56.3 (CH$_2$), 40.5 (N–CH$_3$, br d). Anal. Calcd. for $C_{19}H_{22}BFeNO_2$: C, 62.86; H, 6.11; N, 3.86. Found: C, 65.76; H, 5.89; N, 4.04%. Anal. Calcd. for $C_{19}H_{22}BFeNO_2 \cdot 0.25H_2O$: C, 65.29; H, 5.91; N, 4.01%. HRMS: Found: [M + 2 C$_5$H$_{12}$O$_2$ − 2 H$_2$O]$^+$, 431.1726, $C_{24}H_{30}BFe(III)NO_2^+$ requires 431.1719 (the compound oxidises to Fe(III) upon standing in solution).

Boronic acid **3** could be recrystallised from EtOAc–hexane to give well defined orange crystals of the trimer boroxin (see text) with mp 179–180 °C. Anal. Calcd. for $C_{57}H_{60}B_3Fe_3N_3O_3$: C, 66.14; H, 5.84; N, 4.06. Found: C, 65.66; H, 5.96; N, 3.98%.

1,2-Bis(*N*-methylaminomethyl)ferrocene (6). Ferrocene-1,2-dicarbaldehyde^{35} (500 mg, 2.07 mmol) was dissolved in 4.5 M MeNH$_2$ in EtOH (15 mL) in a N$_2$ atmosphere. The red solution was refluxed for 1 h. After cooling to 0 °C NaBH$_4$ (312 mg, 8.24 mmol) was added in one portion. The mixture was stirred at 0 °C for 30 min and heated to RT for 1 h. The EtOH evaporated and the residue was partitioned between water (40 mL) and ether (40 mL). The aqueous phase was extracted four times with ether (20 mL portions) and the combined ether phase was washed once with brine and dried over Na$_2$SO$_4$. Evaporation yielded 549 mg of an orange oil. The oil was purified on an Al$_2$O$_3$ column (Act. II, 2.5 × 8 cm), eluent ether–ether/MeOH (10%). From eluting with ether two minor fast-running bands were discarded. On changing the eluent to ether–MeOH (9 : 1) the major yellow band eluted slowly off the column. After evaporation an orange oil was obtained. On standing in the freezer overnight, it crystallises into a waxy solid. The yield was 312 mg (55%). Mp 39–42 °C. ^{1}H NMR (CD$_3$OD) δ 4.25 (d, 2H, J = 2.5 Hz, FcH), 4.10 (t, 1H, J = 2.5 Hz, FcH), 4.08 (s, 5H, Fc$_{unsubH}$), 3.63 (d, 2H, J = 13 Hz, N–CH$_2$), 3.41 (d, 2H, J = 13 Hz, N–CH$_2$), 2.86 (s, 6H, N–CH$_3$).^{13}C NMR (CD$_3$OD) δ 85.5, 70.8, 70.1 (Fc$_{unsub}$), 67.7, 50.0 (Fc–CH$_2$), 35.8 (N–CH$_3$). Anal. Calcd. for $C_{14}H_{20}FeN_2$: C, 61.78; H, 7.41; N, 10.29. Found: C, 61.83; H, 7.73; N, 9.97%.

1,2-Bis{*N*-methyl-*N*-[*o*-(dihydroxyboryl)benzyl]aminomethyl}-ferrocene (7). 1,2-Bis(*N*-methylaminomethyl)ferrocene (**6**, 167 mg, 0.61 mmol) was dissolved in dry THF (10 mL) under a N$_2$ atmosphere and cooled to 0 °C. 2,2-Dimethylpropane-1,3-diyl[(*o*-bromomethyl)phenyl]boronate (**12**, 364 mg, 1.29 mmol) was dissolved in dry THF (10 mL) and added drop by drop over 30 min to the above solution by which a precipitate forms. The mixture was stirred for a further 30 min at 0 °C and K$_2$CO$_3$ (dry, powdered) (133 mg, 1.1 equiv) was added and the mixture allowed to stir overnight at RT. The THF was evaporated and the orange residual oil was partitioned between water (15 mL) and EtOAc (25 mL) and deprotected as for boronic acid **3**. Evaporation of the EtOAc yielded an almost pure orange powder (326 mg). Chromatography on an Al$_2$O$_3$ column (Act. II, 2 × 7 cm), eluent CHCl$_3$–MeOH (0 $\longrightarrow$ 5%) was performed to remove small amounts of over-alkylated ammonium com-

pound. The eluate was washed with water to remove MeOH (and hydrolyse any formed methyl esters), dried and evaporated to a few mL, to which pentane was added to precipitate a yellow–orange powder which was isolated by filtration and washed with pentane. After drying the yield of **7** was 233 mg (70%). Analyses suggest varying amounts of anhydride formation between batches. Mp dec. > 200 °C (loses water). ^{1}H NMR (CD$_3$OD) δ 7.60 (d, 2H, J = 6.9 Hz, ArH), 7.29–7.17 (m, 6H, ArH), 4.64 (d, 2H, J = 2.4 Hz, FcH), 4.45 (t, 1H, J = 2.4 Hz, FcH), 4.13 (s, 10H, Fc$_{unsubH}$), 4.18–3.98 (masked CH$_2$-groups, 4H), 2.41 (s, 6H, N-Me). ^{13}C NMR (CD$_3$OD) (C–B not observed due to quadrupolar relaxation) δ 134.6, 129.2, 128.5, 128.1, 72.4, 71.5 (Fc$_{unsub}$), 70.6, 63.9 (N–CH$_2$), 54.5 (N–CH$_2$), 40.3 (N–Me). Anal. Calcd. for $C_{28}H_{34}B_2FeN_2O_4$: C, 62.27; H, 6.35; N, 5.19. Found: C, 65.13; H, 6.13; N, 5.14%. (Anal. Calcd. for $C_{28}H_{34}B_2FeN_2O_4 \cdot 1H_2O$: C, 64.40; H, 6.18; N, 5.37). HRMS: Found: [M + 2 C$_5$H$_{12}$O$_2$ − 4H$_2$O + H]$^+$, 677.3403, $C_{38}H_{51}B_2FeN_2O_4$ requires 677.3384.

1,1′-Bis(*N*-methylaminomethyl)ferrocene (10). Ferrocene-1,1′-dicarbaldehyde^{36} (1.00 g, 4.13 mmol) was dissolved in 4.5 M MeNH$_2$ in EtOH (35 mL) in a N$_2$ atmosphere. The red solution was refluxed for 1 h. After cooling to 0 °C NaBH$_4$ (624 mg, 16.5 mmol) was added in one portion. The mixture was stirred at 0 °C for 30 min and heated to RT for 1 h. The EtOH evaporated and the residue was partitioned between water (50 mL) and ether (50 mL). The aqueous phase was extracted four times with ether (20 mL portions) and the combined ether phase was washed once with brine and dried over Na$_2$SO$_4$. Evaporation yielded 1.10 g of an orange oil. The oil was purified on an Al$_2$O$_3$ column (Act. II, 2.5 × 13 cm), eluent ether–ether/MeOH (10%). A minor fast-running band was discarded and the major yellow band eluted by gradually changing the eluent to ether–MeOH (9 : 1). After evaporation, a red oil was obtained (0.96 g, 86%). ^{1}H NMR (CD$_3$OD) δ 4.17 (4H, t, 1.8 Hz), 4.10 (4H, t, 1.8 Hz), 3.45 (4H, s), 2.32 (3H, s). ^{13}C NMR (CD$_3$OD) δ 86.5, 70.6, 69.7, 51.4 (Fc–CH$_2$), 35.5 (N–CH$_3$). Anal. Calcd. for $C_{14}H_{20}FeN_2$: C, 61.78; H, 7.41; N, 10.29. Found: C, 61.06; H, 7.46; N, 10.02%.

1,1′-Bis{*N*-methyl-*N*-[*o*-(dihydroxyboryl)benzyl]aminomethyl}-ferrocene (11). Synthesized from **10** analogously to **7**. The yield of **11** was 210 mg (63%). Analyses suggest varying amounts of anhydride formation between batches. Mp dec. > 200 °C (loses water). ^{1}H NMR (CD$_3$OD) δ 7.52 (dd, 2H, J = 6.9 Hz, ~1 Hz, ArH), 7.22 (dt, 2H, J = 7.2 Hz, 1.5 Hz, ArH), 7.17 (dt, 2H, J = 7.3 Hz, 1.7 Hz, ArH), 7.07 (d, 2H, J ≈ 7 Hz, ArH), 4.40 (t, 4H, J = 1.8 Hz, FcH), 4.33 (t, 4H, J = 1.8 Hz, FcH), 3.88 (s, 4H, N–CH$_2$), 3.84 (br s, 4H, N–CH$_2$), 2.30 (s, 6H, N–Me). ^{13}C NMR (CD$_3$OD) (C–B not observed due to quadrupolar relaxation) δ 139.5, 133.3, 128.1, 128.0, 126.6, 78.9 (FcC–CH$_2$), 73.4 (FcCH), 71.6 (FcCH), 62.5 (Fc–CH$_2$), 56.0 (Fc–CH$_2$), 40.7 (N–CH$_3$). Anal. Calcd. for $C_{28}H_{34}B_2FeN_2O_4$: C, 62.27; H, 6.35; N, 5.19. Found: C, 65.13; H, 6.26; N, 5.20%. (Anal. Calcd. for $C_{28}H_{34}B_2FeN_2O_4 \cdot 0.9H_2O$: C, 64.20; H, 6.20; N, 5.35). HRMS: Found: [M + 2 C$_5$H$_{12}$O$_2$ − 4 H$_2$O + H]$^+$, 677.3401, $C_{38}H_{51}B_2FeN_2O_4$ requires 677.3384.

References

1 H. Eggert, J. Frederiksen, C. Morin and J. C. Norrild, *J. Org. Chem.*, 1999, **64**, 3846.
2 T. D. James, P. Linnane and S. Shinkai, *Chem. Commun.*, 1996, 281 and references therein.
3 K. R. A. S. Sandanayake, R. Iguchi and S. Shinkai, *J. Chem. Soc., Chem. Commun.*, 1994, 1083.
4 C. J. Ward, P. Patel, P. R. Ashton and T. D. James, *Chem. Commun.*, 2000, 229.
5 M. Takeuchi, T. Mizuno, S. Shinkai, S. Shirakami and T. Itoh, *Tetrahedron: Asymmetry*, 2000, **11**, 3311.
6 K. Tsukagoshi and S. Shinkai, *J. Org. Chem.*, 1991, **56**, 4089.

7 A. Ori and S. Shinkai, *J. Chem. Soc., Chem. Commun.*, 1995, 1771.
8 A. N. J. Moore and D. D. M. Wayner, *Can. J. Chem.*, 1999, **77**, 681.
9 J. C. Norrild and I. Søtofte, *J. Chem. Soc., Perkin Trans. 2*, 2001, 727.
10 J. C. Norrild, *J. Chem. Soc., Perkin Trans. 2*, 2001, 719.
11 T. Burgemeister, R. Grobe-Einsler, R. Grotstollen, A. Mannschreck and G. Wulff, *Chem. Ber.*, 1981, **114**, 3403.
12 S. Toyota and M. Õki, *Bull. Chem. Soc. Jpn.*, 1990, **63**, 1168.
13 S. Toyota, M. Asakura, T. Futawaka and M. Õki, *Bull. Chem. Soc. Jpn.*, 1999, **72**, 1879 and references therein.
14 S. Toyota and M. Õki, *Bull. Chem. Soc. Jpn.*, 1992, **65**, 1832.
15 S. L. Wiskur, J. J. Lavigne, H. Ait-Haddou, V. Lynch, Y. H. Chiu, J. W. Canary and E. V. Anslyn, *Org. Lett.*, 2001, **3**, 1311.
16 G. Wulff, *Pure Appl. Chem.*, 1982, **54**, 2093.
17 T. D. James, K. R. A. S. Sandanayake, R. Iguchi and S. Shinkai, *J. Am. Chem. Soc.*, 1995, **117**, 8982.
18 T. James, S. Sandanayake and S. Shinkai. Fluorescent compound suitable for use in the detection of saccharides. US 5503770, 1996.
19 J. C. Norrild and H. Eggert, *J. Am. Chem. Soc.*, 1995, **117**, 1479.
20 M. Bielecki, H. Eggert and J. C. Norrild, *J. Chem. Soc., Perkin Trans. 2*, 1999, 449.
21 During our work on the synthesis of **3**, **7** and **11** an article describing the synthesis of **17** (Fig. 1) appeared (M. Takeuchi, T. Mizuno, S. Shinkai, S. Shirakami and T. Itoh, *Tetrahedron: Asymmetry*, 2000, **11**, 3311–3322). This molecule, which has a close lying design compared to our sensor molecules, was reported to give a CD response upon glucose addition and $K(\text{D-glucose})/K(\text{L-glucose})$ was reported as 0.77 and $K(\text{D-glucose}) = 685 \text{ M}^{-1}$ at pH = 10.5.
22 H. Kato, K. Kanemitsuya and T. Futagami. Ferrocene-containing fire resistant olefin polymer compositions. JP 63128044 A2, 1988.
23 Non-labelled samples gave a signal-to-noise ratio inadequate to observe the broad absorptions present.
24 W. Yang, H. He and D. G. Drueckhammer, *Angew. Chem., Int. Ed.*, 2001, **40**, 1714 . This communication reports on a new glucose receptor only binding to the pyranose form of glucose.
25 S. Toyota, T. Futawaka, H. Ikeda and M. Õki, *J. Chem. Soc., Chem. Commun.*, 1995, 2499.
26 H. Höpfl, *J. Organomet. Chem.*, 1999, **581**, 129.
27 M. A. Beckett, G. C. Strickland, K. S. Varma, D. E. Hibbs, M. B. Hursthouse and K. M. A. Malik, *J. Organomet. Chem.*, 1997, **535**, 33.
28 W. Kliegel, L. Preu, S. J. Rettig and J. Trotter, *Can. J. Chem.*, 1985, **63**, 509.
29 W. Kliegel, L. Preu, S. J. Rettig and J. Trotter, *Can. J. Chem.*, 1986, **64**, 1855.
30 G. M. Sheldrick, SADABS, Program for Absorption Correction, Bruker AXS Analytical X-ray Systems, Madison, WI, USA, 1996.
31 Siemens, SMART and SAINT, Area-Detector Control and Integration Software, Bruker AXS Analytical X-ray Systems, Madison, WI, USA, 1995.
32 G. M. Sheldrick, SHELXTL95, Bruker AXS Analytical X-ray Systems, Madison, WI, USA, 1995.
33 A. L. Spek, *Acta Crystallogr., Sect. A*, 1990, **46**, C-34.
34 V. I. Boev and A. V. Dombrovskii, *J. Gen. Chem. USSR*, 1977, **47**, 1728.
35 S. I. Goldberg and W. D. Bailey, *J. Am. Chem. Soc.*, 1994, **96**, 6381.
36 U. T. Mueller-Westerhoff, Z. Yang and G. Ingram, *J. Organomet. Chem.*, 1996, **512**, 163.